Real-time monitoring of binding events on a thermostabilized human A$_{2A}$ receptor embedded in a lipid bilayer by surface plasmon resonance

Nicolas Bocquet [a],[*], Josiane Kohler [a], Melanie N. Hug [a], Eric A. Kusznir [a], Arne C. Rufer [a], Roger J. Dawson [b], Michael Hennig [b], Armin Ruf [a], Walter Huber [a], Sylwia Huber [a]

[a] F. Hoffmann-La Roche, Pharma Research and Early Development (pRED), Molecular Design and Chemical Biology, Roche Innovation Center Basel, Grenzacherstrasse 124, Basel CH4070, Switzerland
[b] F. Hoffmann-La Roche, Pharma Research and Early Development (pRED), Discovery Technologies, Roche Innovation Center Basel, Grenzacherstrasse 124, Basel CH4070, Switzerland

ARTICLE INFO

ABSTRACT

Membrane proteins (MPs) are prevalent drug discovery targets involved in many cell processes. Despite their high potential as drug targets, the study of MPs has been hindered by limitations in expression, purification and stabilization in order to acquire thermodynamic and kinetic parameters of small molecules binding. These bottlenecks are grounded on the mandatory use of detergents to isolate and extract MPs from the cell plasma membrane and the coexistence of multiple conformations, which reflects biochemical versatility and intrinsic instability of MPs. In this work ,we set out to define a new strategy to enable surface plasmon resonance (SPR) measurements on a thermostabilized and truncated version of the human adenosine (A$_{2A}$) G-protein-coupled receptor (GPCR) inserted in a lipid bilayer nanodisc in a label- and detergent-free manner by using a combination of affinity tags and GFP-based fluorescence techniques. We were able to detect and characterize small molecules binding kinetics on a GPCR fully embedded in a lipid environment. By providing a comparison between different binding assays in membranes, nanodiscs and detergent micelles, we show that nanodiscs can be used for small molecule binding studies by SPR to enhance the MP stability and to trigger a more native-like behaviour when compared to kinetics on A$_{2A}$ receptors isolated in detergent. This work provides thus a new methodology in drug discovery to characterize the binding kinetics of small molecule ligands for MPs targets in a lipid environment.

1. Introduction

Small molecule interactions with target proteins are of central importance in drug discovery research and are at the heart of many cellular processes such as synaptic transmission regulation, enzyme catalysis, signal transduction and immune response. Membrane proteins are key players in most of these processes and represent an increasing number of potential therapeutic targets of high interest. They also represent the largest family of proteins targeted by marketed small molecules and GPCRs constitute 25% of the all drug-target families of approved medicines [1,2]. Therefore, deciphering and characterizing binding kinetics of candidate drug molecules is a crucial and determinant step in the development of new drugs acting on MPs in order to characterize their mode of action on a specific pathway and their association with and dissociation from target proteins. While the crystal structures of the main classes of GPCRs have been elucidated in presence of agonists, antagonists or inverse agonists within the last decade, greatly increasing our understanding of the molecular mechanisms underlying ligand binding and receptor activation [3–5], studies about the kinetics of these compounds in the cell membrane context remain limited to radioligand assays on membranes and mostly to molecules showing slow dissociation profile.

Surface plasmon resonance (SPR) biosensors represent a well established method to study ligand–protein interactions and enables the accurate assessment of kinetic parameters as association (k_{on}) and dissociation rates (k_{off}), and also dissociation equilibrium constant (K_D), and inhibition constants (IC$_{50}$ and K_i) [6]. SPR also possesses the advantage of being a 'label-free' technology in a sense that the

molecules used as ligands do not require any type of fluorescent or radioactive labelling. Nevertheless, the target protein still needs to be immobilized on the SPR chip surface, a thin gold layer coated with a carboxymethyl dextran matrix. Several methods exist to perform immobilization of target molecules. The widely used amine coupling covalently links the amine groups present on the protein to chemically activated carboxyl groups of the dextran molecules. While very efficient, this coupling can be detrimental for the activity of the immobilized protein due to acidic conditions used by the protein coupling step. For this reason, SPR measurements often require alternative coupling strategies or the presence of tags on the target protein for immobilization purposes. Developing SPR assays with isolated MPs represent a formidable challenge in several aspects. MPs are extracted from the cell membrane with detergents used subsequently throughout the entire purification process and in the SPR running buffer. The detergent micelle is a highly dynamic environment with constant exchanges between the monomeric molecules of detergent and the micelle which represents a non-native environment for the solubilized protein differing significantly from the membrane bilayer. Another difficulty of working with MPs is the high versatility of their conformational states, which are in fast equilibrium. Isolating flexible MPs in detergent might not provide a sufficiently stable environment in which the protein can undergo the full spectrum of its natural conformational landscape or which can lead to stabilization of an inactive state not suitable for binding experiments. For this reason, it is often required to stabilize MPs in a specific conformation by extensive campaigns of mutagenesis combined with thermostability assays. GPCRs are usually stabilized in a specific conformation towards a class of ligands increasing their intrinsic stability and enabling biophysical measurements [7].

In addition, the immobilization of the membrane protein on the SPR biosensor via a tag might also impair the activity of the protein depending on its exact site of immobilization and orientation on the chip surface, which can block the 'extracellular' or 'intracellular' side of the protein. Despite all these bottlenecks, few studies have been successful in demonstrating binding of small ligands on stabilized GPCRs solubilized in detergent by SPR: the neurotensin receptor (NTS1) [8,9], the turkey β1 adrenergic receptor [10,11], the human A_{2A} adenosine receptor [10,12,13] and the native human β2 adrenergic receptor [14] and chemokine receptors CXCR4 and CCR5 solubilized in mixed detergent/lipids micelles [15,16].

In order to circumvent the use of detergent, new solubilizing agents have been developed such as amphipols, synthetic surfactants and block copolymers [17]. Among these new technologies, nanodiscs have emerged as an alternative option and powerful tool, which has already been used for immobilization on an SPR chip of monotopic MPs [18], membrane associated enzymes [19] and the endothelin receptor [20], a class A GPCR but not yet for monitoring of small molecule binding events by SPR. Nanodiscs are size-tunable patches of lipids organized in a lipid bilayer whose hydrophobic edge is encircled by a dimer of Membrane Scaffold Protein (MSP), a derivative from the human Apolipoprotein 1A [21]. Nanodiscs facilitate isolation and stabilization of MPs in a 'membrane-like' environment. They also allow for measuring kinetic parameters by SPR of small molecules on MPs fully embedded in a lipid bilayer, bringing the acquired data closer to what might happen in a native cell membrane. Finally, nanodiscs would enable a complete 'label-free' technology because the target protein itself no longer needs to be tethered to the chip, rather the complex can be immobilized through an engineered MSP. Here we report an SPR-based kinetic study for small molecules binding to the human A_{2A} receptor incorporated in nanodiscs formed by a modified MSP protein carrying a C-terminal C9 tag and immobilized via the 1D4 antibody and via a His tag present on the C-terminus of the receptor. We also compare the binding kinetics of detergent solubilized versus nanodisc reconstituted receptor via two different techniques, SPR and by SPA (scintillation proximity assay). To the best of our knowledge, this is the first report of small molecules binding events monitored by SPR on a human GPCR incorporated in nanodiscs. Our assay provides a novel drug discovery tool to assess the kinetic parameters of small molecules in a lipid environment that closely resembles the lipid contents of cell membranes.

2. Methods

2.1. Protein expression and purification

2.1.1. MSP1D1-C9 protein

The His-TEV-MSP1D1-C9 protein sequence was cloned into a pet28a + plasmid between NcoI and BamHI. The plasmid containing the His-TEV-MSP1D1-C9 coding sequence was transformed in Escherichia coli BL21 (DE3) cells, and the production of the corresponding protein was induced at OD = 0.8 with 0.5 mM IPTG at 20 °C overnight. Cells were disrupted by sonication in the following buffer: Tris 50 mM at pH 7.5; NaCl 300 mM and protease inhibitors (Roche complete EDTA-free, 1 tablet/50 ml); and supernatant was cleared by ultracentrifugation at 176 000 g at 4 °C. The latter was then incubated with TALON cobalt resin (Clontech) at 4 °C for 1 h. The resin was washed batch wise (10 CV) in Tris 50 mM at pH 7.5, NaCl 300 mM and imidazole 10 mM, and the protein was eluted in Tris 50 mM at pH 7.5, NaCl 300 mM and imidazole 400 mM. Imidazole was removed either by dialysis or by desalting columns and the His tag was cleaved by a 10% (w/w) TEV protease digest at room temperature 1–2 h. TEV protease carries a His tag and was then removed by affinity and a short incubation with TALON resin. The final MSP1D1-C9 protein devoid of His tag was collected in the flow-through.

2.1.2. A_{2A} receptor expression and purification

The A_{2A}-rant21 [22] receptor was cloned into a modified pFastBac1 vector and expressed in sf9 cells as a fusion with a GFP-10xHis tag at its C-terminal extremity (after residue 316) separated from the A_{2A} sequence by a 3C protease cleavage site. Cells were infected at a density of 2.10^6 cells/ml at a 0.5% (v/v) virus concentration. Cells were harvested after 72 h of expression by centrifugation in Tris 50 mM at pH 7.5; NaCl 300 mM and protease inhibitors cocktail (ratio biomass/buffer of 1:8) and disrupted by Nitrogen cavitation (30 bar pressure) at 4 °C under constant stirring (350 r.p.m). Cell debris were removed by low-speed centrifugation (20 min at 570 g), and membranes were collected and washed by several cycles of gentle resuspension with a Ultra Turrax and ultracentrigation (25 min at 92 500 g). Membranes were then solubilized in Tris 50 mM at pH 7.5, NaCl 300 mM, imidazole 20 mM, 1% DDM (w/v), 0,1% CHS (w/v) and protease inhibitors (1 tablet per 50 ml of buffer) at a 1.75 ratio (Buffer volume (ml)/Biomass (g)) for 180 min at 4 °C under stirring (300 rpm). The mixture was then subjected to an ultracentrifugation step at 4 °C, and the supernatant was incubated with equilibrated TALON resin at 4 °C overnight under constant stirring. The resin was then poured in a Pharmacia XK16 column and washed in Tris 50 mM at pH 7.5, NaCl 300 mM, imidazole 40 mM, 0.05% DDM and 0.005% CHS, and the protein was finally eluted in Tris 50 mM at pH 7.5, NaCl 300 mM, imidazole 300 mM, 0.05% DDM and 0.005% CHS. The protein was then subjected to a size exclusion chromatography (SEC) on a superdex 200 column run upon the following buffer: HEPES 50 mM at pH 7.3, NaCl 300 mM, 0.05% DDM, 0.005% CHS and TCEP 0.2 mM. The monomeric fractions were pooled, concentrated and flash frozen for storage and further use.

2.2. Nanodisc reconstitution and purification

The lipids POPC and POPG (Avanti Polar Lipids) were dried under an argon beam until creation of a film which was then rehydrated for few hours (typically 3 to 4 h) in 60 mM sodium cholate at a final concentration of 40 mM. POPC and POPG were then mixed in a 3:2 molar ratio, and the solution was extruded by mechanical force with a mini-

extruder (Avanti Polar Lipids). The individual components (A_{2A}-GFP-His:MSP1D1-C9:lipids) were mixed with an optimized molar ratio of 1:3:125, respectively, in HEPES 50 mM at pH 7.3; NaCl 150 mM; 0.05% DDM and 0.005% CHS. The detergent was removed by incubating the mixture with Biobeads (Biorad) for at least 2 h at 4 °C. The beads were discarded, and a His affinity chromatography was performed on the supernatant by incubation of TALON resin by 1 h incubation at 4 °C in order to discard the nanodiscs which were not containing the receptor. The nanodisc complex was then eluted in HEPES 50 mM at pH 7.3, NaCl 300 mM and imidazole 400 mM, and the eluate was run on a Superose 6 column under a HEPES 50 mM at pH 7.3, NaCl 300 mM running buffer. The fractions of the peak corresponding to the nanodisc complex were finally pooled. To check the SEC fractions and/or to screen for reconstitution conditions, FSEC runs were performed on a Superdex 200 5/150 GL (GE healthcare) column with HEPES 50 mM at pH 7.4; NaCl 300 mM as a running buffer.

To produce the empty nanodiscs sample, the same protocol was used but the His tag was then kept on the His-MSP1D1-C9 protein.

2.3. Fluorescence analytical ultracentrifugation

Sedimentation velocity data were recorded at 20 °C (42,000 rpm, with a 60Ti rotor, Spin Analytical SedVel60K centrepieces) using a Beckman Coulter XLI analytical ultracentrifuge equipped with an Aviv fluorescence detection system (excitation at 488 nm, emission at > 505 nm) [23]. The buffer was 50 mM Tris pH 7.5, NaCl 300 mM for A_{2A}-GFP-His in nanodiscs (used at 52 μg/ml with detector gain 2170/PGA 4) and supplemented with 0.05% DDM and 0.005% CHS for A_{2A}-GFP-His in mixed micelles (used at 100 μg/ml with detector gain 1801 V/PGA 4). Data were analysed with the programs Sedfit [24] and Origin (OriginLab) and plotted with GUSSI (http://biophysics.swmed.edu/MBR/software.html) and GraphPad Prism (GraphPad Software). To compare the signal weighted sedimentation coefficients of the two samples, the values were corrected for buffer density and viscosity and reported as $sw_{20,w}$.

2.4. Scintillation proximity assay

For K_D estimation, 15 μl of SPA beads, Ysi-poly-L-lysine-coated beads for the sf9 membranes sample and Ysi copper beads for A_{2A}-GFP-His containing nanodiscs or A_{2A}-GFP-His receptor solubilized in detergent (Perkin-Elmer), 135 μl of the different samples (for membranes: 135 μg per well; for A_{2A}-GFP-His receptor: 0.0052 μg per well and for A_{2A}-GFP-His containing nanodiscs: 0.0524 μg per well) and 50 μl of radioligand ([³H]-SCH 58251) at the corresponding concentrations were dispatched in an Optiplate-96 wells for a final reaction volume of 200 μl. The plate was then shaken for 30 min at 4 °C on a BioShake-IQ prior measurement on a Top Count NXT device at 19 °C. The nonspecific binding signal was estimated by adding large excess of cold ligand in the well (typically 10 μM). As the cold compound was diluted in DMSO, the corresponding concentration of DMSO (1%) was added in the well corresponding to the total binding measurements. Each condition was measured in triplicates and triplicates were averaged to provide a mean value. The nonspecific binding value was then retrieved from the total binding value, giving the specific binding CPM value. A DPM value was furthermore derivatized from the specific binding CPM value as explained in reference [25], and the final quantity of ligand bound (in mmol) per μg of protein added to each well was then normalized to the maximum value of each measurement and plotted against the concentration of hot ligand. Due to the hydrophobic nature of the hot ligand used in this study, the saturation of the signals was not achieved at highest concentrations. This saturation value corresponding to the maximal response has then been extrapolated on each data set individually by a four-parameter nonlinear fit, and only data sets meeting good quality fitting parameters (hill slope, standard deviations and

confidence intervals) in GraphPad Prism (GraphPad Software) were kept and included in the global analysis.

For IC_{50} estimation, 15 μl of SPA beads, 135 μl of the different samples (for A_{2A}-GFP-His receptor: 0.0052 μg per well and for A_{2A}-GFP-His containing nanodiscs: 0.052 μg per well) and 50 μl of [³H]-SCH 58251 at a constant concentration of 6 nM were first mixed in an Optiplate-96 which was shaken for 15 min at 4 °C on a BioShake-IQ. The non-radioactive competitor (ZM 241385 or XAC) was then added to the well at the corresponding concentrations, and the plate was shaken again 15 min prior measurement on Top Count NXT scintillation. The data were treated the same way as for K_D estimation. All final curves were fitted in GraphPad Prism 6 with a stimulation (for K_D) and inhibition (for IC_{50}) nonlinear four parameters fit.

2.5. SPR experiments

Direct binding studies were performed at 18 °C on Biacore 3000 or T200 at flow rate of 50 μl/min in the running buffer composed of Tris 20 mM at pH 7.8, NaCl 350 mM, and supplemented with 0.1% DDM for experiments performed on the detergent solubilized receptor. At the end of each compounds injections, the binding activity and stability of proteins were tested with XAC ligand (at 200 nM). Association and dissociation phases of tested ligands were monitored 120 and 300 s, respectively. The final binding experiment with small molecule ligands was performed in the running buffer supplemented with 0.1% DMSO.

#### 2.5.1. C9 immobilization of the A_{2A} nanodiscs on CM5 or CM7 chip

The mouse Rho 1D4 antibody is first immobilized on CM5 or CM7 chips, previously activated in a 10 min injection of EDC (1-ethyl-3-(3-dimethylaminopropyl)-carbodiimide) 0.2 M/NHS (N-hydroxysuccinimide) 0.05 M mixture and contacted with antibody at concentration of 10 μg/ml diluted in sodium acetate (pH 5.5) buffer until levels of immobilization reached between 15000 and 18000 RU. The chip was then deactivated with a 7 min injection of 1 M ethanolamine, pH 8.0. The A_{2A} nanodiscs were then applied on the chip and captured by the 1D4 antibody to reach typically levels between 4500 and 6500 RU. Empty nanodiscs were immobilized in the same way for reference at levels between 3000 and 4500 RU, considering mass differences of immobilized ligands (nanodiscs with A_{2A} versus empty nanodiscs).

2.5.2. His immobilization of purified A_{2A} and nanodiscs on NTA chip

The NTA chips were preconditioned with three 1-min pulses of EDTA 350 mM at pH 8.3. $NiCl_2$ solution at 500 μM diluted in running buffer was then injected for 3 min. To perform cross-linking of purified A_{2A} or nanodiscs with a dextran layer, flow cells were first activated 5 min with an injection of 0.2 M EDC/0.05 M NHS solution at flow rate of 10 μl/min. Proteins with His tags were then applied on the chip for capturing (A_{2A} nanodiscs: between 4500 and 6800 RU; empty nanodiscs: between 3000 and 4500 RU; and purified A_{2A} around 5000 RU). Empty nanodiscs captured on the sensor surface was used as a reference channel for nanodisc with A_{2A}, whereas activated and deactivated NTA sensor surface was used as a reference channel for purified A_{2A} protein.

2.5.3. Data analysis

The raw sensorgrams corresponding to the receptor in nanodiscs are triple referenced (signals from the reference channels without and with empty nanodiscs are subtracted from the acquired signal in the A_{2A} nanodiscs channels and corrected with a buffer injection) or double referenced for the detergent solubilized receptor. All referenced sensorgrams are analyzed with the BIAevaluation software 3000 (version 4.1) and are fitted with simultaneous k_{on}/k_{off} kinetic fit and 1:1 interaction model including mass transfer.
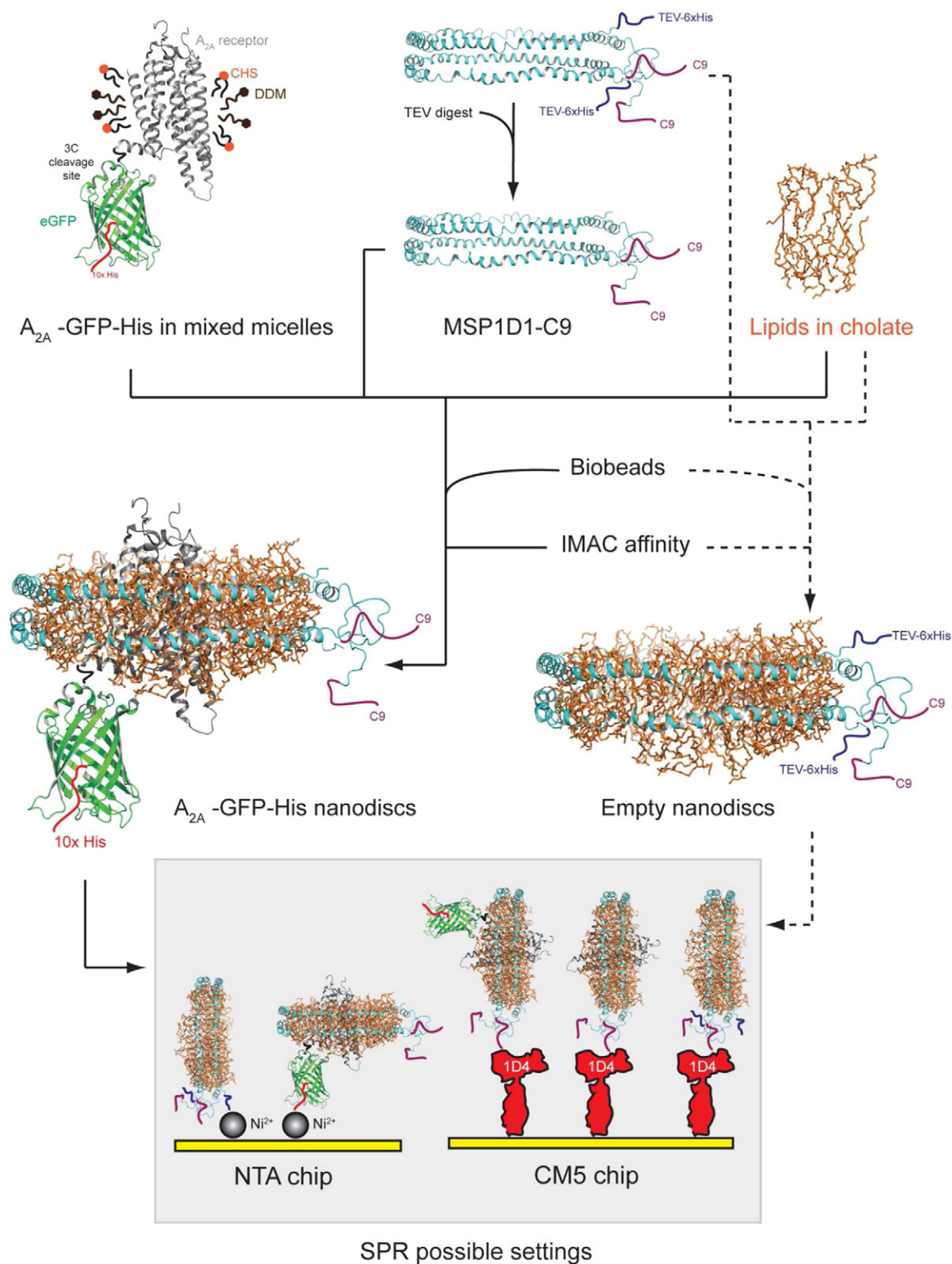
Fig. 1. General strategy for nanodisc production and immobilization on an SPR chip. The receptor is produced as eGFP fusion protein for FSEC protein analytics and for easy monitoring the proper receptor integration in the nanodiscs during their self-assembly. eGFP can be removed at any time thanks to the inserted 3C cleavage site. The different affinity tags on MSP1D1 and A_{2A}-GFP-His allow with a simple affinity chromatography step to remove the nanodiscs which do not contain the A_{2A}-GFP-His receptors or to produce empty nanodiscs for controls and reference purposes. PDB accession codes used to generate the models: A_{2A}, pdb: 3REY from the reference [27], the nanodisc model has been extracted from pdb 3JOO in reference [28] and the eGFP from pdb 2YOG from reference [29].

3. Results

In order to set up and optimize the immobilization methods of GPCR nanodiscs on an SPR chip and subsequent measurements of binding events, we chose to work with a thermostabilized human adenosine A_{2A} receptor carrying four point mutations (A54L, T88A, K122A and V239A) and lacking 96 residues at the C-terminus (rant21 A_{2A}) [22]. The rant21 A_{2A} has been shown to be stabilized in the antagonist

bound form and can be relatively well expressed in several heterologous systems. Several A_{2A} antagonist binding kinetics have been recorded by SPR on the detergent solubilized protein [10,12]. Furthermore, radiolabelled A_{2A} antagonists exist to perform the SPA assays, providing a robust system and a solid reference to optimize the experiments and facilitate the comparison between the two different technologies, SPR and SPA. We fused a GFP at the C-terminus, separated from the A_{2A} sequence by a 3C protease cleavage sequence and followed by a tag comprising 10 histidine residues. This allows us, in a relatively quick manner, to monitor the nanodisc formation by fluorescence size exclusion chromatography (FSEC) [26] and the homogeneity of the final nanodiscs by fluorescence analytical ultracentrifugation while using small amounts of sample. To form the nanodiscs, we expressed and purified a variant of the MSP protein-called MSP1D1—carrying an amino-terminal His tag for purification purposes that can be removed by TEV cleavage, and a C-terminal C9 tag (TETSQVAPA) to immobilize the A_{2A}/nanodisc complex via the 1D4 antibody on the SPR chip (Fig. 1).

3.1. A_{2A} nanodiscs production

To test multiple reconstitution conditions at different molar ratio between the 3 components of the nanodiscs (A_{2A}-GFP-His:MSP1D1-C9:Lipids) or the lipid composition, we adapted a general protocol of nanodiscs self-assembly upon detergent removal followed by a Nickel affinity step to remove nanodiscs, which do not contain the His tagged A_{2A} receptor (Fig. 1). Once eluted, the A_{2A}-GFP-His nanodiscs are subjected to an FSEC screen with two main readouts (1) the elution volume of the A_{2A}-GFP-His fusion protein in absence of detergent and comparison with the elution profile of the A_{2A}-GFP-His run in detergent and (2) the shape of the peak reflecting the sample homogeneity (Fig. 2a). We could identify the most suitable lipid composition, a 3:2 (molar ratio) POPC:POPG mixture supplemented with 0.005% CHS (cholesterol hemisuccinate) and the most suitable molar ratio between A_{2A}-GFP-His: MSP1D1-C9:lipids (1:3:125), leading to a symmetric SEC-peak, which was shown to contain the pure and homogenous co-migrating
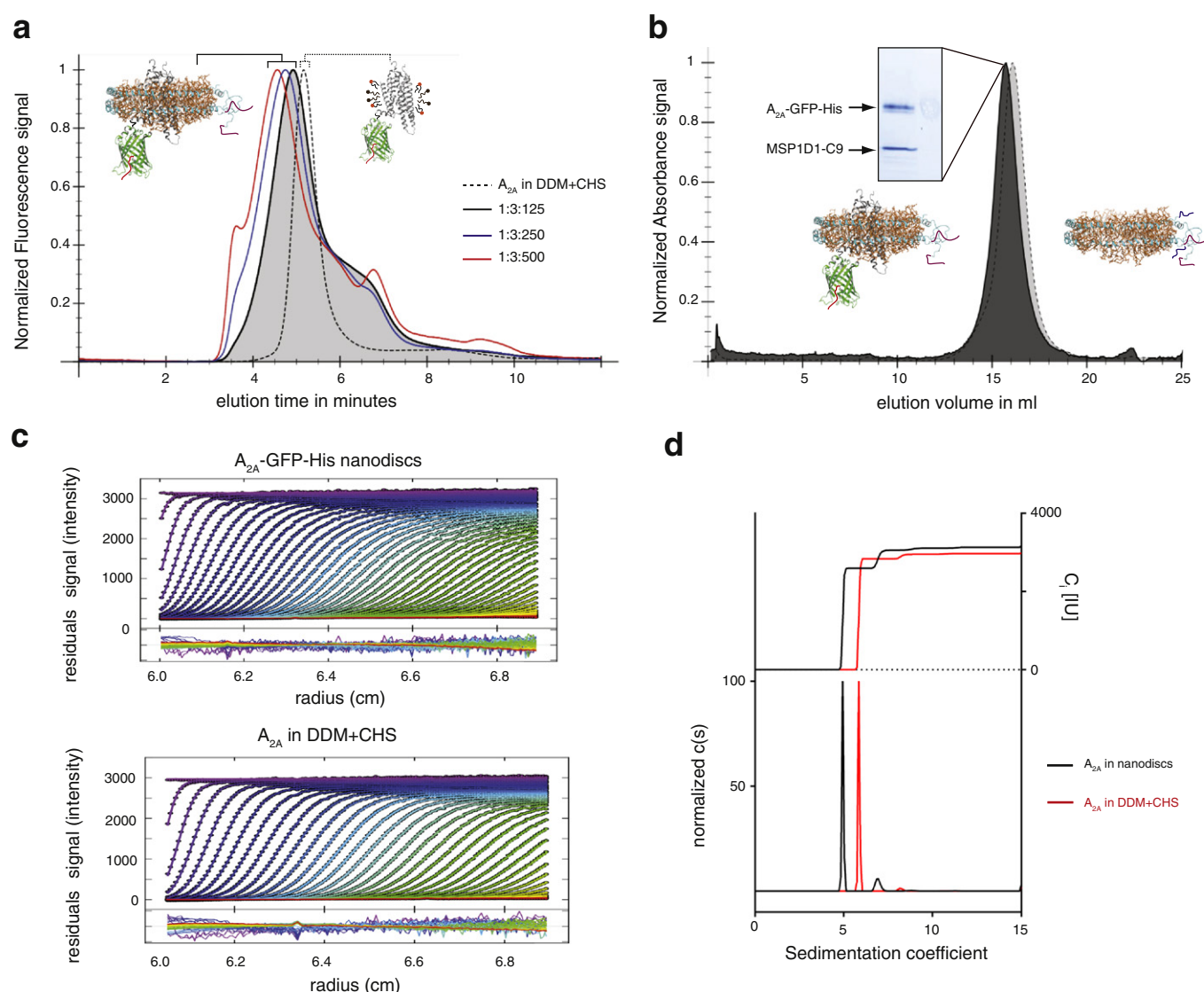

Fig. 2. Purification and characterization of the A_{2A} containing nanodiscs. (a) Fluorescence size exclusion chromatography (FSEC) chromatograms of three samples produced with different A_{2A}-GFP-His:MSP:lipid ratios. The lipids were always POPC:POPG at a 3:2 molar ratio supplemented with 0.005% CHS. For reference the chromatogram obtained with the detergent solubilized A_{2A}-GFP-His is shown as a black dashed line. (b) Final preparative size exclusion chromatography purification (superose 6) of the A_{2A}-GFP-His nanodiscs (solid black line shaded with dark grey). The insert corresponds to the peak fractions pooled and loaded on an SDS–PAGE. The empty nanodisc reference is displayed as a dashed black line shaded with light grey. (c) Sedimentation boundaries (dots, fluorescence signal vs. radial position, every third scan is shown for clarity), fits to data (solid lines) and residuals (bottom panels) of A_{2A}-GFP-His in nanodiscs and detergent mixed micelles. (d) Sedimentation coefficient distributions c(s) for the data from panel c, the upper panel shows the integrated distributions (total loading signal).

proteins by SDS–PAGE (Fig. 2b and Supp Fig. 1). We observed partial aggregation of the A_{2A}-GFP-His receptor upon overlipidation as revealed by the increasing amount of fluorescent material in the void volume of the column (Fig. 2a) at ratios above 1:3:250. This condition could be extrapolated to produce larger amounts of A_{2A}-GFP-His nanodiscs. To confirm the homogeneity of the samples, we performed fluorescence analytical ultracentrifugation with A_{2A}-GFP-His incorporated in MSP1D1-C9 nanodiscs and A_{2A}-GFP-His in detergent mixed micelles (DDM 0.05% + CHS 0.005%). A total of 82% of the total fluorescence signal (integrated main peak) can be attributed to A_{2A}-GFP-His in nanodiscs ($sw_{20,w} = 5.6$ S), 95% in the case of the A_{2A}-GFP-His solubilized in detergent mixed micelles ($sw_{20,w} = 6.5$ S). Thus, both preparations can be considered monodisperse. Using a partial specific volume of vbar = 0.821 ml/g derived from the weight-fractions of one A_{2A}-GFP-His receptor, two MSP1D1-C9 molecules and an estimated 75 POPC/POPG lipid molecules in the nanodisc complex, a molecular weight of 163 kDa can be calculated from the sedimentation velocity data [9,30]. This corresponds well to the expected molecular weight of 168 kDa of this complex and shows that our nanodisc preparation contains monomeric A_{2A}-GFP-His receptor.

3.2. Binding parameters assessed by SPA

A scintillation proximity assay (SPA) is a fast way to determine kinetic and binding parameters and is widely used in drug discovery [25]. Normally, SPA is applied on purified MPs or full cells containing the receptor. Nevertheless, the β2 adrenergic receptor [31] and the bacterial leucine transporter [32] reconstituted in nanodiscs or reconstituted high-density lipoprotein (rHDL) have already been subjected to SPA, demonstrating the feasibility of the technique to determine K_D, association and dissociation rate constants of radioligands on MPs inserted in an artificial lipid bilayer. SPA with the tritiated [^{3}H] SCH 58251 A_{2A} antagonist was used to experimentally determine its dissociation equilibrium constant in four different assay formats: membranes of *sf9* cells expressing the A_{2A}-GFP-His construct, the A_{2A}-GFP-His receptor purified in detergent supplemented or not with 0.005% CHS and the A_{2A}-GFP-His receptor reconstituted in nanodiscs (Fig. 3a). SPA has the great advantage to enable measurements on membranes of *sf9* cells by using poly-L-lysine-coated Ysi beads. K_D of [^{3}H]SCH 58251 on A_{2A}-GFP-His inside the cell membrane was determined with a value of 0.93 ± 0.57 nM. The K_D measured on isolated A_{2A} receptor in DDM and CHS and on A_{2A}-GFP-His receptor reconstituted in nanodiscs immobilized via the A_{2A} His tag to Ysi copper beads were in the similar nanomolar range: $K_{D\ DDM} = 7.98 \pm 3.94$ nM, $K_{D\ DDM\text{-}CHS} = 6.15 \pm 6.09$ nM and $K_{D\ nanodiscs} = 14.86 \pm 5.68$ nM. Due to the unspecific binding of [^{3}H]SCH 58251 ligand at increased concentrations of hot ligand, it was not possible to acquire reliable saturation values. These have therefore been extrapolated by a nonlinear four-variable parameters fit strategy. As the calculated K_D value for A_{2A}-GFP-His solubilized in detergent is within the confidence intervals of the K_D obtained for the A_{2A}-GFP-His receptor in nanodiscs, we observe no significant difference in affinity of SCH 58251 for A_{2A}-GFP-His receptor once extracted from the membrane, but the affinity is approximately 10 times better when A_{2A}-GFP-His is still embedded in the native membrane. Finally, competition assays (Fig. 3b and c) allowed us to determine IC_{50} of ZM 241385 and XAC (Xanthine Amine Congener) on A_{2A}-GFP-His in DDM + CHS ($IC_{50\ ZM\ 241385} = 12.17$ nM; $IC_{50\ XAC} = 236.4$ nM) and in nanodiscs ($IC_{50\ ZM\ 241385} = 52.44$ nM; $IC_{50\ XAC} = 819.4$ nM), two antagonists which have been cocrystallized with A_{2A} receptor [27]. The values determined with the SPA assay on the rant-21 A_{2A} mutant in this study (Table 1) are overall in good agreement with the previously published values obtained with other radiobinding methods [22] and on the wild-type protein [33,34]. To decipher the kinetic parameters in deeper details, we analysed the different samples in an SPR analysis.
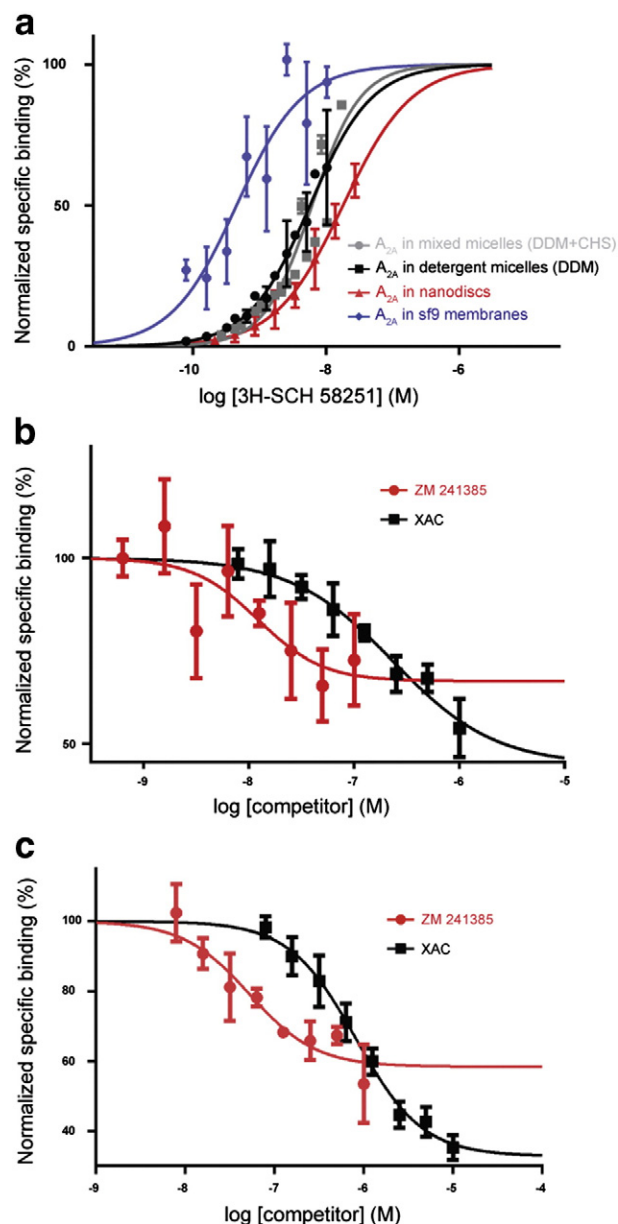
Fig. 3. SPA binding assay with [^{3}H]-SCH 58251. (a) K_D estimation of different A_{2A}-GFP-His receptor preparations. The normalized specific binding CPM signals are expressed in percentage of the maximal predicted saturation plateau value and plotted against the concentration range of tritiated SCH 58251. The lines correspond to the mathematical fit of the experimental data (four variables nonlinear fit). The error bars correspond to the standard deviation calculated from 3 independent experiments. Blue diamonds: A_{2A}-GFP-His in native *sf9* cell membranes. Grey squares: A_{2A}-GFP-His solubilized in DDM detergent with CHS. Black squares: A_{2A}-GFP-His solubilized in DDM detergent without CHS. Red triangles: A_{2A}-GFP-His reconstituted in nanodiscs. (b) Competition assay with ZM 241385 and XAC with A_{2A}-GFP-His solubilized in detergent in panel b or reconstituted in nanodiscs in panel c.

3.3. Real-time monitoring of small molecules binding by SPR

We first assessed the antagonist binding activity of A_{2A}-GFP-His isolated in DDM micelles by immobilization on NTA chip as represented on Fig. 4a. We determined the binding constants by SPR of three antagonists (ZM 241385, SCH 58251 and XAC) in a running buffer containing 0.1% DDM (Fig. 4b, c and d). The protein binding activity level calculated from the sensorgrams obtained with the detergent solubilized receptor is 52% (with an estimated molecular mass of 80 kDa). The binding parameters derived from these measurements are listed in Table 2 and

Table 1
Binding parameters of A_{2A} antagonists determined by SPA at 19 °C.

Compound	MW (Da)	logP	SPA							
			Reference in membranes		Detergent (DDM 0.05% + CHS 0.005%)			Nanodiscs		
			K_D (nM)	k_{off} (s-1)	K_D (nM)	IC50 (nM)	k_{off} (s-1)	K_D (nM)	IC50 (nM)	k_{off} (s-1)
XAC	428	1.62	ND	ND	ND	236.4	ND	ND	819.4	ND
ZM 241385	337	2.52	ND	ND	ND	12.17	ND	ND	52.44	ND
SCH 58251	345	3.02	0,93 ± 0.57	1.57E-02	7,98 ± 3.94	ND	0.85E-02	14,86 ± 5.68	ND	0.84E-02

are in close agreement with a previous study performed on the same A_{2A} construct [10]. A_{2A}-GFP-His nanodiscs were then immobilized via the His tag present on the carboxy terminal tail of the GFP fused to the receptor by direct affinity coupling on nickel NTA chip, reaching levels of immobilization typically around 6000 RU (Fig. 4a). This is a reasonable amount for small molecules binding events detection on large objects as nanodiscs as the amplitude of the recorded signal is proportional to the ratio between the molecular size of the binder (in this study, ranging from 337 to 428 Da) and the size of the target (estimated around 163 kDa for the A_{2A}-GFP-His nanodiscs). Furthermore, this capturing method allows immobilization of empty nanodiscs on a reference channel and to cross-link the pre-captured nanodisc complex to the chip by amine coupling (Fig. 4e, f, g and h). Cross-linking of nanodiscs

on the biosensor produces more stable baseline and avoid dissociation of protein from sensor surface as previously reported on detergent solubilized A_{2A} receptor [10]. Thus, it is possible to monitor significantly higher binding responses when compared to experiments with non-cross-linked nanodiscs. In this configuration, the application of antagonists solutions elicited responses between 5 and 10 RU of amplitude allowing accurate characterization of binding kinetics of the 3 antagonists. Repetitive injections of concentration series of each compound generate reproducible and saturable signals demonstrating the robustness of the assay setup. In addition, the nanodisc environment greatly increases the stability of the A_{2A} receptor as it could be stored for months at 4 °C, and data were recorded for several weeks with the same chip without significant loss of activity (approximately 80% active
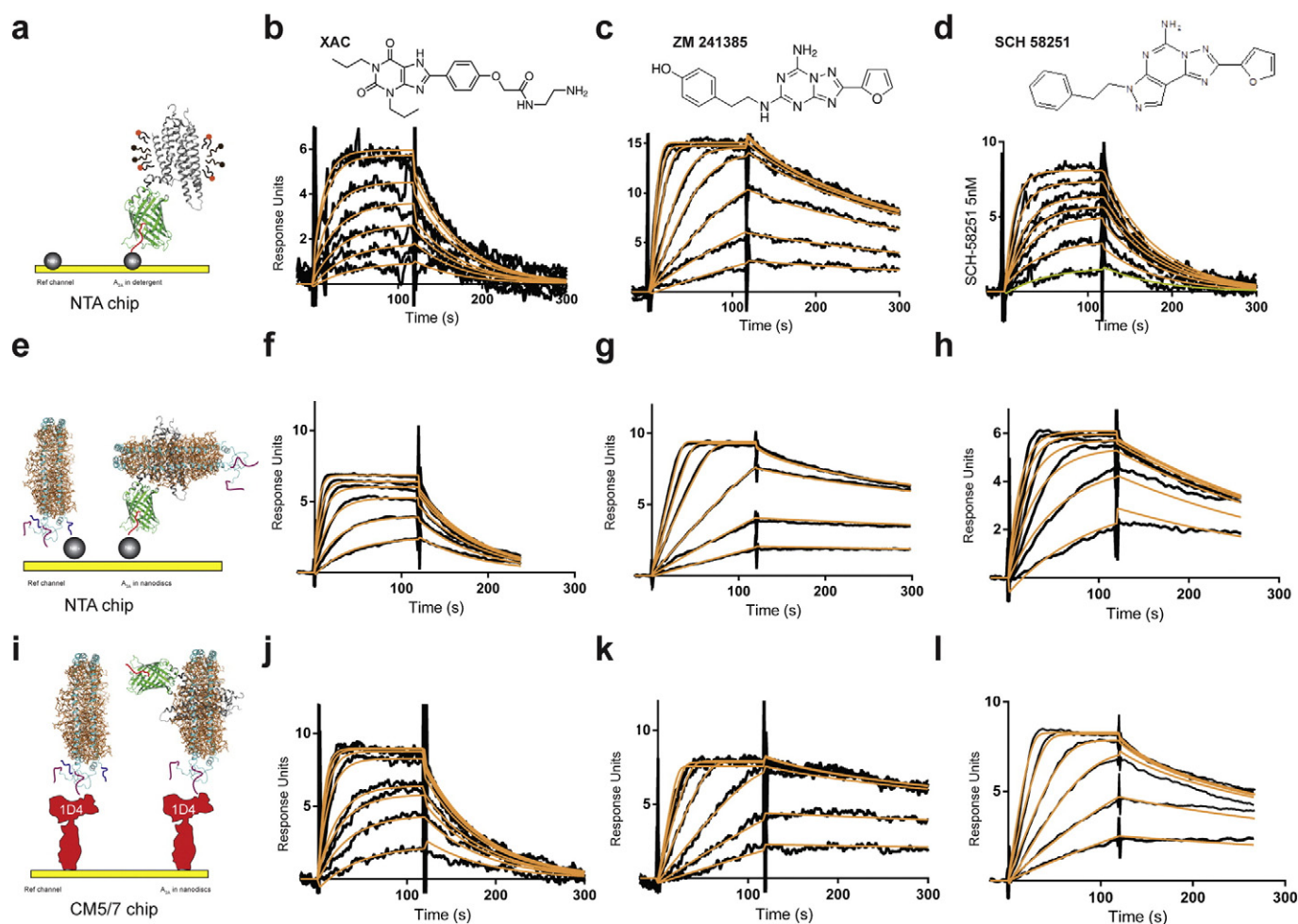
Fig. 4. Kinetic analysis at 18 °C of A_{2A} antagonists by SPR. (a, b, c and d) Dose–response curves obtained with the detergent solubilized His tag captured receptor as shown on panel a for XAC (5-10-15-20-40-60 and 80 nM), ZM 241385 (2-4-8-16-25-50-75 and 100 nM) and SCH 58251 (5-10-20-30-40-60 and 100 nM) respectively. (e, f, g and h) The same kinetic analysis performed on A_{2A} containing nanodiscs immobilized through the C9 epitope present on the MSP1D1 protein as shown in the inset panel e. (i, j, k and l) Kinetic analysis performed on A_{2A} containing nanodiscs immobilized through the His tag located on the receptor as shown in panel i.

Table 2
Binding parameters of A_{2A} antagonists determined by SPR at 18 °C.

Compound	MW (Da)	SPR								
		Detergent (DDM 0.1%)			Nanodiscs					
					C9 immobilization			His immobilization		
		k_{on} (M-1 s-1)	k_{off} (s-1)	K_D (nM)	k_{on} (M-1 s-1)	k_{off} (s-1)	K_D (nM)	k_{on} (M-1 s-1)	k_{off} (s-1)	K_D (nM)
XAC	428	7.36E+05 ± 3.28E+05	1.82E−02 ± 5.23E−03	24.70 ± 11.11	1.57E+06 ± 1.02E+06	1.57E−02 ± 1.64E−02	9.90 ± 2.13	2.09E+06 ± 2.20E+06	1.46E−02 ± 1.43E−02	6.98 ± 1.07
ZM241385	337	3.30E+06 ± 1.43E+06	5.99E−03 ± 1.18E−03	1.82 ± 0.49	2.48E+07 ± 8.92E+06	3.55E−03 ± 6.66E−04	0.14 ± 0.16	1.10E+07 ± 1.50E+07	3.11E−03 ± 2.84E−03	0.28 ± 0.0051
SCH 58251	345	7.34E+05 ± 1.05E+06	1.60E−02 ± 7.21E−03	21.7 ± 7	3.67E+06 ± 1.36E+06	7.62E−03 ± 2.74E−03	1.98 ± 0.46	1.42E+06 ± 2.57E+05	3.82E−03 ± 1.92E−04	2.70 ± 0.70

protein, Supplementary Fig. 2). We did not observe any influence of the cross-linking on protein binding activity and on binding constants. We next immobilized the nanodisc complex via the MSP1D1 protein. After the covalent immobilization of the 1D4 antibody on CM5 or CM7 chip by classical amine coupling, the A_{2A} nanodiscs were captured via the C9 epitope by the antibody (Figs. 1 and 4i). A similar high level of immobilization (6000–7000 RU) was reached, and the biosensor was equilibrated with the running buffer until achieving of stable baseline. We could also attach C9 containing empty nanodiscs on a reference channel and substract the reference sensorgram from the A_{2A}-GFP-His nanodiscs sensorgram. Fig. 4 summarizes the dose–response sensorgrams obtained for the three compounds on detergent solubilized A_{2A}-GFP-His receptor (Fig. 4b,c and d), A_{2A}-GFP-His nanodiscs immobilized via the receptor (Fig. 4e,f g and h) and via the MSP1D1 protein (Fig. 4i, j, k and l) and the binding constants are reported on Table 2. While binding constants are very similar for XAC ($K_{D\ A2A\text{-}GFP\text{-}his/XAC} = 24.7 \pm 11.11$ nM and $K_{D\ nanodiscs/XAC} = 9.97 \pm 2.13$ nM with highly similar association and dissociation rates), for ZM 241385 ($K_{D\ A2A\text{-}GFP\text{-}His/ZM} = 1.82 \pm 0.49$ nM and $K_{D\ nanodiscs/ZM} = 0.14 \pm 0.16$ nM) and SCH 58251 ($K_{D\ A2A\text{-}GFP\text{-}His/SCH} = 21.7 \pm 7$ nM and $K_{D\ nanodiscs/SCH} = 1.98 \pm 0.46$ nM), the K_D values are one order of magnitude shifted to lower values for the receptor reconstituted in nanodiscs. This difference could not be detected by the SPA assay where K_D for SCH 58251 are all in the nanomolar range. These discrepancies in K_D can be almost completely explained by differences in k_{on} rates, which are faster (around 10 fold) for the receptor incorporated in nanodiscs compared to the detergent solubilized receptor (Table 2). We tried to test if these differences stem from the presence of CHS in the A_{2A}-GFP-His nanodiscs, which is absent in the running buffer of the SPR experiments on the detergent solubilized protein, but were unable to perform convincing measurements once the running buffer containing 0.1% DDM was supplemented with 0.001% CHS, pointing out the fact that ZM 241385 and even more SCH 58251 do not behave well in presence of CHS. It is important to note that no binding signal has been detected on empty nanodiscs (reference channel), indicating that there is no detectable pre-binding of the antagonists to the nanodiscs. The results obtained on the detergent solubilized receptor are in good agreement with the previously reported binding constants [10].

4. Discussion

To address the question whether detergent purified GPCRs have similar kinetic behaviour than membrane embedded GPCRs, we developed nanodisc-based SPR assay to determine small molecules binding parameters on A_{2A} receptor inserted in a membrane-like environment. In this study, we established and compared various nanodiscs immobilization strategies, either via the receptor through the C-terminally located His tag or via the nanodisc itself through a C9 epitope located on the MSP protein. We determined kinetic constants of small molecules on the A_{2A} receptor embedded in those lipid bilayer nanodiscs by SPR, and compared them to the kinetics measured on detergent solubilized receptors. We also performed and determined binding parameters by SPA, a radiobinding assay, that we compared to values obtained with SPR. We detected some deviations and differences between the receptor isolated in detergent or reconstituted in nanodiscs which might have important significance for drug discovery.

4.1. Observed kinetic parameters are independent on the immobilization procedure

Overall, we assessed the influence of GPCR immobilization on antagonist binding kinetics. Nanodiscs were designed to allow immobilization of A_{2A} nanodiscs on the chip via the nanodiscs or via a tag on A_{2A} in order to check whether attaching the receptor directly on the chip (with or without cross-linking) via its own tag could affect the binding kinetics. Table 2 shows that neither on- nor off-rates or K_D were significantly affected by the different immobilization procedures (Fig. 4). Moreover, the presence of the GFP-His tag on the receptor does not have detectable influence on binding constants (Supplementary Fig. 2), highlighting the fact that the main influencing parameter on kinetic rates is the membrane environment. In agreement with this idea, we observed lower K_D values for SCH 58251 by SPA on membranes of cells expressing A_{2A}-GFP-His and for ZM 241385 and SCH 58251 on the A_{2A}-GFP-His nanodisc samples by SPR. Even if we cannot completely rule out the possibility of an influence of the way of anchoring the sample on the SPA beads via the negatively charged lipids present in the cell membrane, the native membrane provides obviously the best environment for the binding activity of the A_{2A} receptor. Nevertheless, the SPA experiment requires labelled compounds, and membrane samples cannot be handled with the SPR technology. Hence, the nanodisc represents a minimal lipidic environment enabling label-free SPR measurements with both 'extracellular' and 'intracellular' sides accessible for ligand binding.

4.2. Nanodiscs further stabilize the inserted A_{2A} receptor

A very important parameter for SPR experiments is the stability of a protein as defined as the time it remains active. Stability is one of the main limiting factors when working with isolated MP whose ligands have slow kinetics parameters or when performing SPR screening activities. We showed in this study that the A_{2A} receptor incorporated in nanodiscs possesses increased binding activity (80% when inserted in nanodiscs versus 52% in detergent micelles) and stability allowing SPR data acquisition on the same chip without regeneration for two to three weeks at least while the activity of the detergent solubilized A_{2A} is almost completely lost after 80 h. The nanodisc sample could also be stored at 4 °C for 6 months prior immobilization on the chip without significant loss of activity (Supplementary Fig. 2). This represents a clear advantage of the nanodisc technology over detergent-GPCR-micelles as it could enable larger SPR screens on GPCR reconstituted in lipid bilayer. While any MP can in principle be inserted into nanodiscs highlighting the universality of the method, a stabilized version of the MP might

still be a prerequisite to allow sufficient active binding site immobilization on the biosensor chip in order to generate a detectable signal. This is a limitation of the method in case wild-type GPCRs are absolutely required for kinetic studies as they might be too unstable. To determine whether this methodology is applicable to native MPs would require further investigations.

4.3. Influence of the nanodisc environment on kinetics parameters

One of the striking features observed in this study is that association rates for two compounds (ZM 241385 and SCH 58251) appear significantly faster (one order of magnitude) when the A_{2A} receptor is inserted in nanodiscs resulting in stronger affinities than those measured on detergent solubilized receptors. One hypothesis to this observation could be that the presence of a lipid bilayer modifies the access pathway of the ligand to the receptor. It has been shown on the β1 adrenergic receptor that drug-membrane protein association rates are governed by the 'membrane affinity' of the compound [35] that leads to a partial partitioning inside the lipid bilayer. The non-homogenous distribution of a compound with a higher local concentration in the membrane close to the receptor gives rise to a higher receptor bound fraction and consequently to apparently increased association rates. Interestingly, the most drastic deviations are observed with ZM 241385. For this compound, indeed, the observed association rate on A_{2A} nanodiscs is 10 times faster than for the detergent solubilized receptor. This observation is also true for SCH 58251 but to a lower extent. This behaviour correlates with the lipophilicity of the compounds as reflected by the logP values. SCH 58251 (logP = 3.02) and ZM 241385 (logP = 2.52) have most likely a good propensity to partition inside the lipid bilayer formed by the nanodisc assembly. XAC whose binding constant on detergent or nanodiscs solubilized receptors are very similar has a lower logP value (1.62) and potentially partition less within the lipid bilayer. In order to test whether the observed K_D discrepancies could be only explained by differences in k_{on} rates, we estimated the k_{off} rates of [^{3}H]SCH 58251 on A_{2A} receptors still embedded in native membranes and compared it to detergent and nanodiscs solubilized receptors by time resolved SPA (Table 2 and Supplementary Fig. 3). The obtained k_{off} values are very similar to those measured with SPR ($k_{off/nanodiscs/SPR} = 0.76 \times 10^{-2}$ s^{-1} and $k_{off/detergent/SPR} = 1.60 \times 10^{-2}$ s^{-1}). Moreover, nanodiscs and detergent solubilized A_{2A} receptors do not show significant k_{off} rates differences ($k_{off/membranes/SPA} = 1.57 \times 10^{-2}$ s^{-1}; $k_{off/nanodiscs/SPA} = 0.84 \times 10^{-2}$ s^{-1} and $k_{off/detergent/SPA} = 0.85 \times 10^{-2}$ s^{-1}). These data confirm that the main factor affecting the final K_D is the association rate and not the dissociation rate, at least for SCH 58251 antagonist. Although this is not a definitive proof and we can rule out an additional effect of the introduced mutations on the kinetic behaviour of the receptor in a lipid environment, these observations point out the fact that the physico-chemical properties of ligands and their ability to partition inside lipid bilayer are crucial parameters having an important impact on the local 'micro kinetic' of membrane proteins. An additional piece of explanation could be the presence of CHS in the lipid composition of the nanodiscs. It has been shown that cholesterol binds to A_{2A} in the surrounding of helix VI and might act as an allosteric modulator [36]. It indeed displaces the side chain of the N253 towards the ligand present in the binding pocket (in this case ZM 241385) creating additional hydrogen bonding and therefore potentially increasing the affinity of ZM 241385 for the A_{2A} receptor. For all these aspects, nanodiscs represent a wonderful tool, which was missing in the SPR field, to decipher these effects and this study shows that they are good mimics of the cell membrane, at least for kinetic studies, in recapitulating some of the properties of the membrane. Nevertheless, more systematic investigations are clearly required to better describe the influence of lipophilicity of ligands as well as the effects of lipids on the kinetic.

4.4. Potential impacts of nanodisc-based SPR on drug discovery

The first important impact is on the determination of 'real or improved' kinetic parameters. To get closer to what really happens inside a cell membrane when a ligand binds to a membrane protein can greatly help in bridging different levels of experimentation within the drug discovery pipeline. An enhanced accuracy in kinetic constants for a given compound and taking into account the effect of the lipid environment on the binding properties might, if not fully explain, at least highlight some discrepancies between *in vitro* assays on a detergent solubilized membrane protein and the results of cell assays in which plasma membrane has a great influence on the binding activity of the same membrane protein. These advantages can be extrapolated to screening activities like fragment based screen by SPR on human integral membrane proteins incorporated in nanodiscs. The presence of a lipid bilayer and its influence on the membrane protein functionality might end up with different or more biologically relevant hits. The output of such a screen could be directly compared with what has already been done on detergent solubilized GPCRs [11].

5. Conclusion

In this study, we demonstrated that SPR experiments can be performed in a universal (applicable to all membrane proteins) and complete 'label-free' manner that raises the possibility to study the influence of agonistic or antagonistic ligands on the binding of G proteins or β-arrestin as extracellular and intracellular sides of the GPCR are accessible in this current setup. Kinetic studies on influence of signal transducers binding on ligands affinities, potencies, efficacies or on effects of allosteric modulators as lipids can therefore be envisioned. The reverse setup could also be tested by screening which G protein and therefore which pathway is activated upon binding of a given ligand. Finally, the nanodiscs allow the use of detergent-free conditions, increase tremendously the stability of the protein inserted in and, therefore, represent a very good substitute to native membrane.

Supplementary data to this article can be found online at http://dx.doi.org/10.1016/j.bbamem.2015.02.014.

Author contributions

N.B. designed the experiments, managed the project, performed protein purification, nanodisc reconstitution, SPA and pilot SPR experiments. J.K, S.H and M.N.H performed, optimized and analyzed SPR experiments. E.A.K and A.C.R performed fluorescence analytical ultracentrifugation experiments and analysis. R.J.D provided the A_{2A} constructs and equipments for protein purification. M.H, A.R, W.H and S.H supervised the project. N.B wrote the manuscript with inputs of W.H, S.H, A.R, R.J.D and A.C.R.

Conflict of interest

Authors declare no conflicts of interest.

References

[1] A.L. Hopkins, C.R. Groom, The druggable genome, Nat. Rev. Drug Discov. 1 (2002) 727–730.

[2] C.S. Tautermann, GPCR structures in drug design, emerging opportunities with new structures, Bioorg. Med. Chem. Lett. (2014) 4073–4079.

[3] A.J. Venkatakrishnan, X. Deupi, G. Lebon, C.G. Tate, G.F. Schertler, M.M. Babu, Molecular signatures of G-protein-coupled receptors, Nature 494 (2013) 185–194.

[4] D.M. Rosenbaum, S.G.F. Rasmussen, B.K. Kobilka, The structure and function of G-protein-coupled receptors, Nature 459 (2009) 356–363.

[5] K. Hollenstein, C. de Graaf, A. Bortolato, M.-W. Wang, F.H. Marshall, R.C. Stevens, Insights into the structure of class B GPCRs, Trends Pharmacol. Sci. 35 (2014) 12–22.

[6] R.L. Rich, D.G. Myszka, Advances in surface plasmon resonance biosensor analysis, Curr. Opin. Biotechnol. 11 (2000) 54–61.

[7] N. Robertson, A. Jazayeri, J. Errey, A. Baig, E. Hurrell, A. Zhukov, C.J. Langmead, M. Weir, F.H. Marshall, The properties of thermostabilised G protein-coupled receptors (StaRs) and their use in drug discovery, Neuropharmacology 60 (2011) 36–44.

[8] P.J. Harding, T.C. Hadingham, J.M. McDonnell, A. Watts, Direct analysis of a GPCR-agonist interaction by surface plasmon resonance, Eur. Biophys. J. 35 (2006) 709–712.

[9] S. Inagaki, R. Ghirlando, J.F. White, J. Gvozdenovic-Jeremic, J.K. Northup, R. Grisshammer, Modulation of the interaction between neurotensin receptor NTS1 and Gq protein by lipid, J. Mol. Biol. 417 (2012) 95–111.

[10] R.L. Rich, J. Errey, F. Marshall, D.G. Myszka, Biacore analysis with stabilized G-protein-coupled receptors, Anal. Biochem. 409 (2011) 267–272.

[11] J.A. Christopher, J. Brown, A.S. Doré, J.C. Errey, M. Koglin, F.H. Marshall, D.G. Myszka, R.L. Rich, C.G. Tate, B. Tehan, T. Warne, M. Congreve, Biophysical fragment screening of the β1-adrenergic receptor: identification of high affinity arylpiperazine leads using structure-based drug design, J. Med. Chem. (2013) 3446–3455.

[12] A. Zhukov, S.P. Andrews, J.C. Errey, N. Robertson, B. Tehan, J.S. Mason, F.H. Marshall, M. Weir, M. Congreve, Biophysical mapping of the adenosine A2A receptor, J. Med. Chem. (2011) 4312–4323.

[13] D. Chen, J.C. Errey, L.H. Heitman, F.H. Marshall, A.P. Ijzerman, G. Siegal, Fragment screening of GPCRs using biophysical methods: identification of ligands of the adenosine A2A receptor with novel biological activity, ACS Chem. Biol. (2012) 2064–2073.

[14] T. Aristotelous, S. Ahn, A.K. Shukla, S. Gawron, M.F. Sassano, A.W. Kahsai, L.M. Wingler, X. Zhu, P. Tripathi-Shukla, X.P. Huang, J. Riley, J. Besnard, K.D. Read, B.L. Roth, I.H. Gilbert, A.L. Hopkins, R.J. Lefkowitz, I. Navratilova, Discovery of β2 adrenergic receptor ligands using biosensor fragment screening of tagged wild-type receptor, ACS Med. Chem. Lett. 4 (2013) 1005–1010.

[15] I. Navratilova, M. Dioszegi, D.G. Myszka, Analyzing ligand and small molecule binding activity of solubilized GPCRs using biosensor technology, Anal. Biochem. 355 (2006) 132–139.

[16] I. Navratilova, J. Sodroski, D.G. Myszka, Solubilization, stabilization, and purification of chemokine receptors using biosensor technology, Anal. Biochem. (2005) 271–281.

[17] J.-L. Popot, Amphipols, nanodiscs, and fluorinated surfactants: three nonconventional approaches to studying membrane proteins in aqueous solutions, Annu. Rev. Biochem. 79 (2010) 737–775.

[18] J.M. Glueck, B.W. Koenig, D. Willbold, Nanodiscs allow the use of integral membrane proteins as analytes in surface plasmon resonance studies, Anal. Biochem. 408 (2011) 46–52.

[19] A. Das, J. Zhao, G.C. Schatz, S.G. Sligar, R.P. Van Duyne, Screening of type I and II drug binding to human cytochrome P450-3A4 in nanodiscs by localized surface plasmon resonance spectroscopy, Anal. Chem. 81 (2009) 3754–3759.

[20] D. Proverbio, C. Roos, M. Beyermann, E. Orban, V. Doetsch, F. Bernhard, Functional properties of cell-free expressed human endothelin A and endothelin B receptors in artificial membrane environments, Biochim. Biophys. Acta 1828 (2013) 2182–2192.

[21] T.H. Bayburt, S.G. Sligar, Membrane protein assembly into nanodiscs, FEBS Lett. 584 (2010) 1721–1727.

[22] F. Magnani, Y. Shibata, M.J. Serrano-Vega, C.G. Tate, Co-evolving stability and conformational homogeneity of the human adenosine A2a receptor, Proc. Natl. Acad. Sci. U. S. A. (2008) 10744–10749.

[23] J.S. Kingsbury, T.M. Laue, Fluorescence-detected sedimentation in dilute and highly concentrated solutions, Methods Enzymol. 492 (2011) 283–304.

[24] P. Schuck, Size-distribution analysis of macromolecules by sedimentation velocity ultracentrifugation and Lamm equation modeling, Biophys. J. 78 (2000) 1606–1619.

[25] D. Harder, D. Fotiadis, Measuring substrate binding and affinity of purified membrane transport proteins using the scintillation proximity assay, Nat. Protoc. 7 (2012) 1569–1578.

[26] T. Kawate, E. Gouaux, Fluorescence-detection size-exclusion chromatography for precrystallization screening of integral membrane proteins, Structure 14 (2006) 673–681.

[27] A.S. Doré, N. Robertson, J.C. Errey, I. Ng, K. Hollenstein, B. Tehan, E. Hurrell, K. Bennett, M. Congreve, F. Magnani, C.G. Tate, M. Weir, F.H. Marshall, Structure of the adenosine A2A receptor in complex with ZM241385 and the xanthines XAC and caffeine, Structure (2011) 1283–1293.

[28] J. Frauenfeld, J. Gumbart, E.O.V.D. Sluis, S. Funes, M. Gartmann, B. Beatrix, T. Mielke, O. Berninghausen, T. Becker, K. Schulten, R. Beckmann, Cryo-EM structure of the ribosome–SecYE complex in the membrane environment, Nat. Struct. Mol. Biol. 18 (2011) 614–621.

[29] A. Royant, M. Noirclerc-Savoye, Stabilizing role of glutamic acid 222 in the structure of enhanced green fluorescent protein, J. Struct. Biol. 174 (2011) 385–390.

[30] S. Inagaki, R. Ghirlando, R. Grisshammer, Biophysical characterization of membrane proteins in nanodiscs, Methods 59 (2013) 287–300.

[31] C. Fiez-Vandal, L. Leder, F. Freuler, D. Sykes, S.J. Charlton, S. Siehler, U. Schopfer, M. Duckely, HDL-like discs for assaying membrane proteins in drug discovery, Biophys. Chem. 165 (2012) 56–61.

[32] M.L. Nasr, S.K. Singh, Radioligand binding to nanodisc-reconstituted membrane transporters assessed by the scintillation proximity assay, Biochemistry (2013) 4–6.

[33] A. Uustare, A. Vonk, A. Terasmaa, K. Fuxe, A. Rinken, Kinetic and functional properties of [3H]ZM241385, a high affinity antagonist for adenosine A2A receptors, Life Sci. (2005) 513–526.

[34] K.A. Bennett, B. Tehan, G. Lebon, C.G. Tate, M. Weir, F.H. Marshall, C.J. Langmead, Pharmacology and structure of isolated conformations of the adenosine A2A receptor define ligand efficacy, Mol. Pharmacol. (2013) 949–958.

[35] D.A. Sykes, C. Parry, J. Reilly, P. Wright, R.A. Fairhurst, S.J. Charlton, Observed drug-receptor association rates Are governed by membrane affinity: the importance of establishing "micro-pharmacokinetic/pharmacodynamic relationships" at the β2-adrenoceptor, Mol. Pharmacol. (2014) 608–617.

[36] W. Liu, E. Chun, A.A. Thompson, P. Chubukov, F. Xu, V. Katritch, G.W. Han, C.B. Roth, L.H. Heitman, A.P. IJzerman, V. Cherezov, R.C. Stevens, Structural basis for allosteric regulation of GPCRs by sodium ions, Science (2012) 232–236.